ISSN 1674-1056
http://cpb.iphy.ac.cn
http://iopscience.iop.org/cpb
中国物理 B
Chinese Physics
中国物理
Chinese Physics B

Contribution of terahertz waves to near-field radiative heat transfer between graphene-based hyperbolic metamaterials

Qi-Mei Zhao(赵启梅), Tong-Biao Wang(王同标), De-Jian Zhang(张德建), Wen-Xing Liu(刘文兴), Tian-Bao Yu(于天宝), Qing-Hua Liao(廖清华), Nian-Hua Liu(刘念华)

Citation: Chin. Phys. B . 2018, 27(9): 094401. **doi:** 10.1088/1674-1056/27/9/094401

Journal homepage: http://cpb.iphy.ac.cn; http://iopscience.iop.org/cpb

What follows is a list of articles you may be interested in

Reconstruction model for temperature and concentration profiles of soot and metal-oxide nanoparticles in a nanofluid fuel flame by using a CCD camera

Guannan Liu(刘冠楠), Dong Liu(刘冬)

Chin. Phys. B . 2018, 27(5): 054401. **doi:** 10.1088/1674-1056/27/5/054401

Optical response of tunable terahertz plasmon in a grating-gated graphene transistor

Bo Yan(闫博), Jingyue Fang(方靖岳), Shiqiao Qin(秦石乔), Yongtao Liu(刘永涛), Li Chen(陈力), Shuang Chen(陈爽), Renbing Li(李仁兵), Zhen Han(韩震)

Chin. Phys. B . 2017, 26(9): 097802. **doi:** 10.1088/1674-1056/26/9/097802

Broadband tunability of surface plasmon resonance in graphene-coating silica nanoparticles

Zhe Shi(史哲), Yang Yang(杨阳), Lin Gan(甘霖), Zhi-Yuan Li(李志远)

Chin. Phys. B . 2016, 25(5): 057803. **doi:** 10.1088/1674-1056/25/5/057803

Simultaneous reconstruction of temperature distribution and radiative properties in participating media using a hybrid LSQR–PSO algorithm

Niu Chun-Yang, Qi Hong, Huang Xing, Ruan Li-Ming, Wang Wei, Tan He-Ping

Chin. Phys. B . 2015, 24(11): 114401. **doi:** 10.1088/1674-1056/24/11/114401

Spectral enhancement of thermal radiation by laser fabricating grating structure on nickel surface

Liu Song, Liu Shi-Bing

Chin. Phys. B . 2015, 24(5): 054401. **doi:** 10.1088/1674-1056/24/5/054401

Contribution of terahertz waves to near-field radiative heat transfer between graphene-based hyperbolic metamaterials*

Qi-Mei Zhao(赵启梅)[1], Tong-Biao Wang(王同标)[1,†], De-Jian Zhang(张德建)[1], Wen-Xing Liu(刘文兴)[1], Tian-Bao Yu(于天宝)[1], Qing-Hua Liao(廖清华)[1], and Nian-Hua Liu(刘念华)[2]

[1] *Department of Physics, Nanchang University, Nanchang* 330031, *China*
[2] *Institute for Advanced Study, Nanchang University, Nanchang* 330031, *China*

(Received 16 February 2018; revised manuscript received 15 May 2018; published online 28 August 2018)

Hyperbolic metamaterials alternately stacked by graphene and silicon (Si) are proposed and theoretically studied to investigate the contribution of terahertz (THz) waves to near-field radiative transfer. The results show that the heat transfer coefficient can be enhanced several times in a certain THz frequency range compared with that between graphene-covered Si bulks because of the presence of a continuum of hyperbolic modes. Moreover, the radiative heat transfer can also be enhanced remarkably for the proposed structure even in the whole THz range. The hyperbolic dispersion of the graphene-based hyperbolic metamaterial can be tuned by varying the chemical potential or the thickness of Si, with the tunability of optical conductivity and the chemical potential of graphene fixed. We also demonstrate that the radiative heat transfer can be actively controlled in the THz frequency range.

Keywords: radiative heat transfer, graphene, hyperbolic metamaterials

PACS: 44.40.+a, 78.67.Wj, 81.05.Xj **DOI:** 10.1088/1674-1056/27/9/094401

1. Introduction

Radiative heat transfer has aroused a great deal of interest in the past few decades; many studies focus on the near-field radiative heat transfer due to its potential applications in thermal imaging,[1–4] radiative cooling,[5] near-field thermophotovoltaics,[6,7] and thermal energy conversion.[8] The near-field radiative heat transfer that can exceed the blackbody limit has been extensively studied in various systems.[6–12] In the presence of resonant surface modes, such as surface phonon polaritons (SPhPs) and surface plasmon polaritons (SPPs), the heat transfer between two bodies in the near-field regime can be enhanced significantly. The materials that can support SPhPs[11] or SPPs[12] were employed to control the heat transfer in several studies. In addition, the hyperbolic mode (HM) excited by hyperbolic metamaterial (HMM) often covers a wider frequency range than SPhP or SPP, which is limited to a small frequency band around its resonance frequency. Therefore, the near-field radiative heat transfer between hyperbolic materials has also been investigated by many researchers.[9,10]

Terahertz (THz) wave, a type of electromagnetic wave with a frequency in a range from 0.1 THz to 10 THz, has received increasing attention because of its promising applications in spectroscopy,[13,14] imaging,[15] bio-sensing,[16] communication,[17] etc. In the past few years, many attempts have been made to improve the absorption of THz waves, which facilitates the development of THz detectors,[18,19] thermal emitters, and sensors.[20,21] In addition, the THz technology has potential applications in near-field microscopy and thermal management.[22] Furthermore, the contribution of THz waves to near-field radiation transfer is also an interesting subject of investigation.[23–25] However, there are few natural materials except graphene[26,27] capable of supporting THz SPhP or SPP, which plays an important role in enhancing radiative heat transfer. Graphene, a newly emerged two-dimensional (2D) mono-layered carbon-atom-arranged material, has received a great deal of attention in the field of nanophotonics due to its excellent optical properties.[28] Graphene can support SPPs in a frequency range from THz to mid-infrared frequencies due to its unique Dirac band structure. Furthermore, when graphene is connected to other dielectric materials,[29] the hyperbolic modes can appear at THz or mid-infrared frequencies by tuning its chemical potential. Therefore, the HMM with a hyperbolic band can be constructed to enhance the radiation transfer in THz and near-field frequency regimes.

In this paper, we theoretically investigate the near-field radiative heat transfer between HMMs each of which is periodically stacked by graphene and silicon (Si) in the THz region. On the one hand, we make full use of the advantage that the hyperbolic mode covers a wider frequency range than the surface resonance mode. The proposed structure can enhance the near-field radiative heat transfer in a wider frequency range. On the other hand, when the suitable width of Si and chemical potential of graphene are selected, the radiative heat transfer of THz waves between graphene-based HMMs can be

*Project supported by the National Natural Science Foundation of China (Grant Nos. 11704175, 11664024, and 61367006).
†Corresponding author. E-mail: tbwang@ncu.edu.cn
© 2018 Chinese Physical Society and IOP Publishing Ltd

enhanced remarkably compared with that between graphene-covered Si bulks. Furthermore, the near-field radiative heat transfer in the THz frequency regime between graphene-based hyperbolic metamaterials can be tuned actively by controlling the chemical potential of graphene.

2. Theoretical model

As have been studied in Refs. [30] and [31] , the HMM is a special class of uniaxial anisotropic material in which the dispersion relation of the electromagnetic wave is given by the following equation:[32]

$$\frac{q^2}{\varepsilon_\perp}+\frac{k_z^2}{\varepsilon_\parallel}=\frac{\omega^2}{c^2}, \tag{1}$$

where $\varepsilon_\perp$ and $\varepsilon_\parallel$ are the permittivities for the electric field components that are parallel and perpendicular to the optical axis, respectively; q is the parallel component of the wave vector; k_z is the component of the wave vector along the z direction; and ω is the angular frequency of the electromagnetic waves. For HMM, the sign of $\varepsilon_\perp$ is different from that of $\varepsilon_\parallel$. In other words, the dispersion function describes not an ellipse but a hyperbolic dispersion curve. When $\varepsilon_\perp<0$ and $\varepsilon_\parallel>0$ ($\varepsilon_\perp>0$ and $\varepsilon_\parallel<0$), the HMM supports the hyperbolic modes that are evanescent in the vacuum gap and can propagate inside the hyperbolic material when $q>\sqrt{\varepsilon_\perp}\omega/c$.

A periodic multilayer structure composed of graphene and Si as shown in Fig. 1(a) is considered. The permittivities in the directions perpendicular and parallel to the graphene surface can be described by the effective medium theory (EMT). The graphene-based periodic structure in the long wavelength regime can be modeled with uniaxial effective permittivity by the following expressions:[33]

$$\varepsilon_\parallel=\frac{t_g\varepsilon_g+d\varepsilon_d}{t_g+d}, \tag{2}$$

$$\varepsilon_\perp=\frac{\varepsilon_g\varepsilon_d(t_g+d)}{t_g\varepsilon_d+d\varepsilon_g}, \tag{3}$$

where ε_g is the equivalent permittivity of graphene, which is defined as $\varepsilon_g=1+\mathrm{i}\sigma\eta_0+k_0+t_g$, σ is the optical conductivity of graphene, and $\eta_0\approx 377\ \Omega$ is the impedance of air. $k_0=\omega/c$ is the vacuum wave vector with the speed of light c, and $t_g=0.5$ nm represents the effective thickness of graphene. $\varepsilon_d=11.56$ is the dielectric constant of Si in THz frequency,[34] and d is the thickness of Si. In the low frequency range, the interband conductivity of graphene can be ignored, so the optical conductivity σ of graphene can be expressed as $\sigma=\frac{\mathrm{i}e^2\mu}{\pi\hbar^2(\omega+\mathrm{i}\tau^{-1})}$,[35] where e is the electron charge, $\hbar$ is the reduced Planck's constant, ω is the angular frequency of the THz wave, μ is the chemical potential of graphene determined by the carrier concentration $n_0=(\mu/\hbar v_F)^2/\pi$, and the density n_0 of the carriers can be controlled by the gate voltage or chemical doping. τ is the relaxation time, which is due to the losses caused by the electron impurity, electron defect, and electron–phonon scattering. Equations (2) and (3) indicate that the perpendicular component of permittivity $\varepsilon_\perp$ is approximately equal to that of Si, whereas the parallel component of permittivity $\varepsilon_\parallel$ changes with frequency. The proposed graphene-based multilayer structure can exhibit the property of HMM in some frequency range when suitable parameters are selected.

The effective permittivities of the graphene-based HMMs are shown in Fig. 1(b). This figure shows a hyperbolic band with $\varepsilon_\parallel<0$ and $\varepsilon_\perp>0$ for a p-polarized wave when the frequency is lower than 7.62 THz. The frequency for $\varepsilon_\parallel=0$ is defined as the critical frequency. The real part of $\varepsilon_\parallel$ is always negative in the hyperbolic region, while at higher frequencies, the real part of $\varepsilon_\perp$ is positive and tends to coincide with. Moreover, the location of the critical frequency can be actively controlled by modulating the chemical potential as shown in Fig. 1(c). This figure shows that the critical frequency shifts toward higher frequencies with the chemical potential increasing. Therefore, the hyperbolic band can be tuned flexibly. In addition, the effective permittivity can also be tuned by changing the thickness of the dielectric layer. The variations of the real part of $\varepsilon_\parallel$ with frequency for different dielectric thickness are shown in Fig. 1(d) at a fixed chemical potential of $\mu=0.1$ eV. The critical frequency moves to lower frequencies when the thickness of the dielectric layer increases, resulting in a narrow hyperbolic band.

To describe the near-field radiative heat flux, the radiative transfer coefficient (RTC) $h(D)$ of THz wave between HMMs, which are assumed to be at a local thermal equilibrium, is calculated from the following equation:[36]

$$h(D)=\frac{1}{\pi^2}\int_0^\infty \mathrm{d}\omega\frac{\partial\Theta(\omega,T)}{\partial T}\int_0^\infty s(\omega,q)\,\mathrm{d}q, \tag{4}$$

where $\Theta(\omega,T)=\hbar\omega/(\mathrm{e}^{\hbar\omega/k_BT}-1)$ is the mean energy of the Planck oscillator with k_B being the Boltzmann constant. The integrand in Eq. (4) is generally called the spectral transfer function (STF), which can be given by the following equation:

$$H(\omega,D)=\frac{1}{\pi^2}\int_0^\infty s(\omega,q)\,\mathrm{d}q, \tag{5}$$

where

$$s(\omega,q)=q\frac{\mathrm{Im}(R_1^j(\omega))\,\mathrm{Im}(R_2^j(\omega))\,\mathrm{e}^{-2|k_{0z}|D}}{|1-R_1^j(\omega)R_2^j(\omega)\,\mathrm{e}^{2\mathrm{i}k_{0z}D}|^2}$$

is an exchange function. The wave vector in the z direction is $k_{0z}=\sqrt{\omega^2/c^2-q^2}$. $R_i^j(\omega)$ ($i=1,\ 2;\ j=\mathrm{s},\mathrm{p}$) is the reflection coefficient from the surface of HMM for j-polarized wave. The contribution of s-polarized wave to radiative transfer can be neglected in the near-field regime. Therefore, only a p-polarized wave is considered in this paper. The reflection

coefficient for the p-polarized wave can be given by the following equation:

$$R^{\mathrm{p}} = \frac{\varepsilon_{\parallel} p_0 - p_{\mathrm{m}}}{\varepsilon_{\parallel} p_0 + p_{\mathrm{m}}}, \tag{6}$$

where $p_0 = \sqrt{1-\kappa^2}$, $p_{\mathrm{m}} = \sqrt{\varepsilon_{\parallel} - \varepsilon_{\parallel}\kappa^2/\varepsilon_{\perp}}$, and $\kappa = cq/\omega$ is a normalized quantity with $\kappa > 1$ for the evanescent waves.

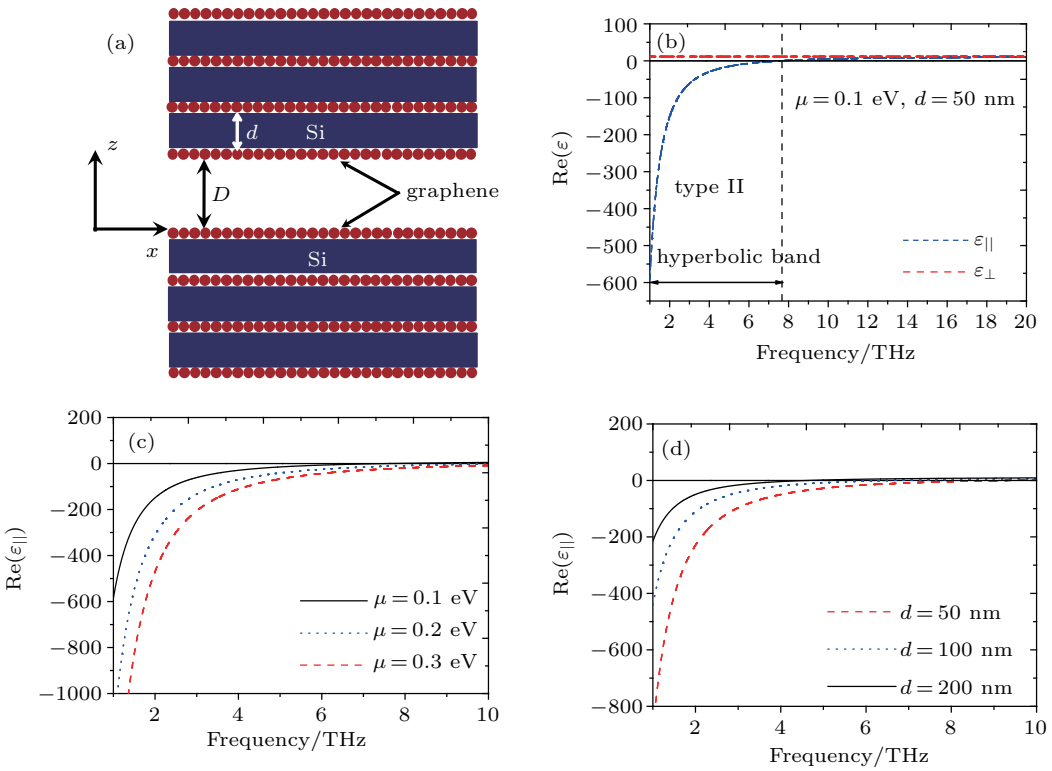


Fig. 1. (color online) (a) Schematic of the THz wave transfer between two graphene-based HMMs separated by a vacuum gap D. (b) The real part of the effective permittivities parallel ($\varepsilon_{\parallel}$) and perpendicular ($\varepsilon_{\perp}$) to the surface of graphene as a function of frequency. The width of Si is $d = 50$ nm, and the chemical potential of graphene is $\mu = 0.1$ eV. (c) Variation of the real part of $\varepsilon_{\parallel}$ with frequency for different chemical potentials with $d = 50$ nm. (d) Variation of the real part of $\varepsilon_{\perp}$ with frequency for different thickness with $\mu = 0.1$ eV.

3. Results and discussion

Figure 2 shows the contours of exchange function $s(\omega, q)$ for graphene-covered silicon bulk and HMM in the left and right panels, respectively. The chemical potentials of graphene are $\mu = 0.05$, $\mu = 0.1$, and $\mu = 0.15$ eV and eV from top to bottom panels. The frequency ranges are limited in the THz region. The width of Si is still set to be $d = 50$ nm. Although each exchange function exhibits a bright region, the characteristics of the modes in the left and right panels are different. For the graphene-covered structure, the contribution to the exchange function is from graphene-supported surface plasmons (SPs), whereas for HMM, this contribution is from HM. The SPs and HM appear in different frequency regions even if the chemical potentials are the same for both configurations, which is due to the fact that the HM excited by the HMM often covers a wider frequency range than SPhPs or SPPs whose frequency is limited to its resonance frequency. In addition, the chemical potential has a distinct effect on the SPs and HM, leading to a shift toward higher frequencies when the chemical potential increases. The exchange function can represents the electromagnetic wave tunneling probability between two HMMs (or graphene-covered Si bulks). It depends on both the frequency and the dimensionless wave vector component along the x direction. However, to further compare the advantages of different configurations, we display the STF for two different configurations in the following study.

In Fig. 3, the STFs are shown as a function of frequency for different chemical potentials. To compare the STF of HMM with that of graphene-covered Si bulk, we define a dimensionless parameter $\Gamma = H(\omega)/H_{\mathrm{g-Si}}(\omega)$, where $H(\omega)$ and $H_{\mathrm{g-Si}}(\omega)$ are the STFs of HMMs and graphene-covered Si, respectively. In our calculation, the vacuum gap is fixed to be 150 nm, and the thickness of Si is maintained at 50 nm to satisfy the validity of EMT. The black solid, red dashed, and blue dotted lines correspond to the cases with chemical potentials of 0.05 eV, 0.1 eV, and 0.15 eV, respectively. For each chemical potential selected, a peak appears in the STF curve as shown in Fig. 3. Each value of Γ is smaller than 1.0 at lower frequency; thus, the radiative transfer between graphene-covered Si bulks is larger than that between HMMs in such a frequency range. However, when the frequency increases, the value of Γ increases very rapidly. The maximum value of Γ can reach 3.5 when $\mu = 0.15$ eV. Therefore, the

radiative heat transfer can be significantly enhanced between HMMs than that between graphene-covered Si bulks. However, when the frequency is beyond the THz range, the difference in curve among the three different chemical potentials almost disappears. In addition, as the chemical potential increases, the peak moves toward higher frequencies with an increasing value. Therefore, the radiative transfer of THz wave might be tuned by the chemical potential. The STF does not drop to zero over the THz band, which is because of the weak contribution of other surface waves.

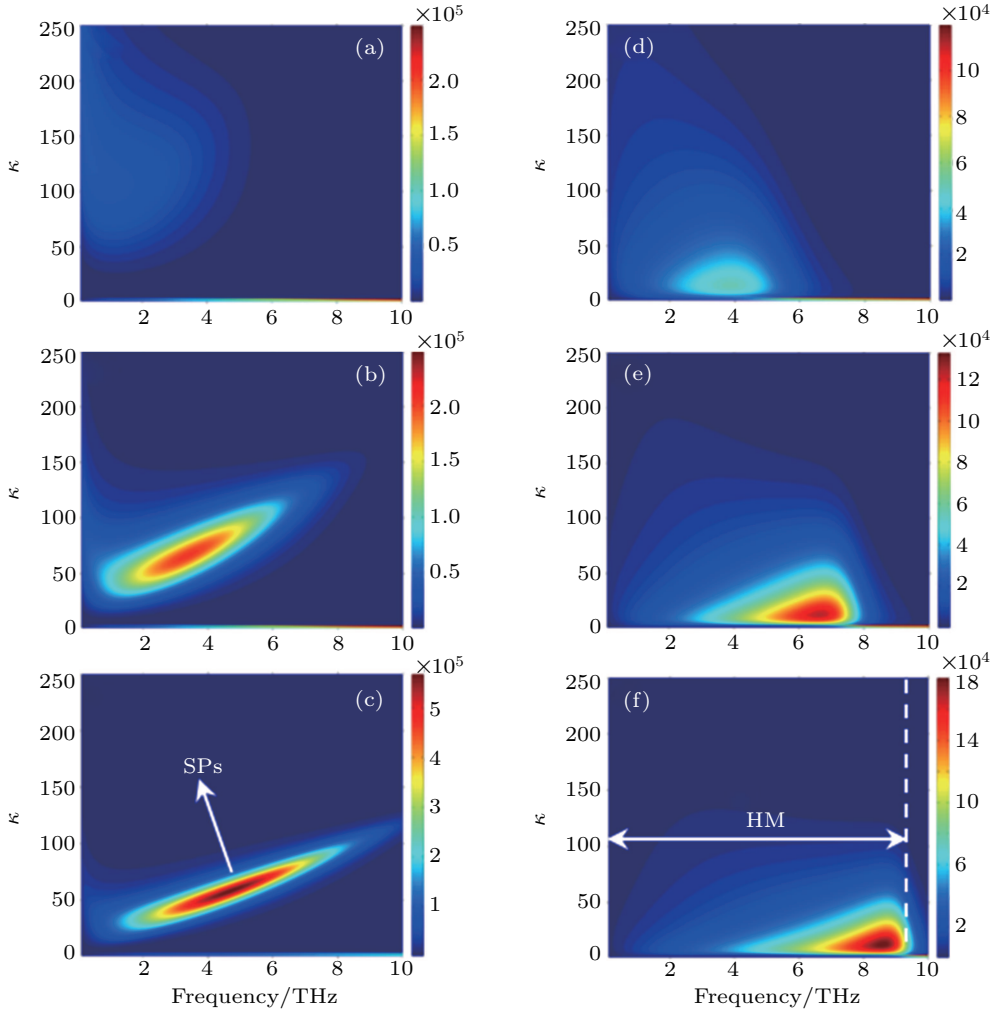


Fig. 2. (color online) Exchange function $s(\omega, q)$ for different chemical potentials of (a)–(c) graphene-covered semi-infinite structure and (d)–(f) graphene-based HMM. Chemical potential is $\mu = 0.05$ eV ((a) and (d)), 0.1 eV ((b) and (e)), and 0.15 eV ((c) and (f)). The vacuum gap is fixed to be $D = 150$ nm, and the thickness of Si is set to be $d = 50$ nm.

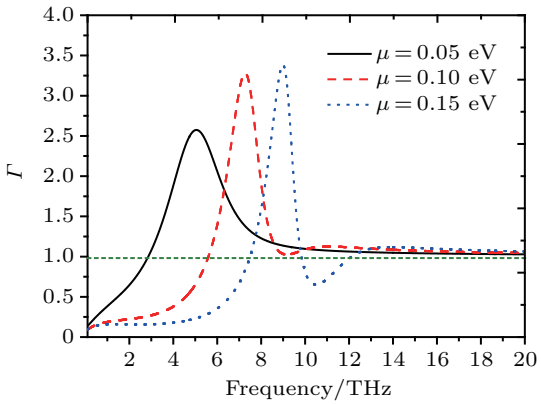


Fig. 3. (color online) Plots of ratio between STFs of HMM and graphene-covered Si bulk versus frequency for different chemical potentials. The vacuum gap is set to be 150 nm, and the thickness of Si is 50 nm in HMM.

We have analyzed qualitatively the radiative transfer between HMMs using STF. In addition, we find that the radiative transfer can be larger or less for the HMMs than that for the graphene-covered Si bulk in different frequency ranges. The properties of graphene are determined by its chemical potential; thus, the chemical potential significantly affects the property of graphene-based HMM. Here, we study the RTC through the total THz frequency range (from 0.1 THz to 10 THz). Similarly, we define a dimensionless parameter γ_μ, which is the ratio of the RTC of HMMs to the RTC of graphene-covered Si bulk, that is $\gamma_\mu = h(\mu)/h_{\mathrm{g-Si}}(\mu)$. The thickness of Si in HMM is 50 nm in Eq. (4). Figure 4 shows the γ_μ as a function of chemical potential for different vac-

uum gaps. The values of γ_μ for vacuum gaps $D = 300$ and $D = 1000$ nm are displayed with black solid and red dashed curves, respectively. The value of γ_μ first increases and then decreases as the chemical potential increases for each case. The values of γ_μ reach the maximum values at 0.05 eV and 0.075 eV for vacuum gaps of 300 and 1000 nm, respectively. The value of γ_μ is larger for vacuum gap 300 nm than that for 1000 nm when the chemical potential is less than 0.085 eV; after which, the value of γ_μ is smaller for $D = 300$ nm than that for $D = 1000$ nm. For most of the chemical potential values in our study, γ_μ is larger than 1.0. Therefore, the radiative transfer between HMMs is stronger than that between graphene-Si structures. However, when the chemical potential is larger than 0.134 eV, the radiative transfer of THz wave between HMMs cannot catch up with that between graphene-covered Si structures when the vacuum gap is 300 nm. For vacuum gap $D = 1000$ nm, the value of γ_μ is smaller than 1.0 when the chemical potential is larger than 0.148 eV. Therefore, HMMs can enhance the near-field radiative transfer of THz wave by selecting a suitable chemical potential. Furthermore, we can actively control the radiative transfer by tuning the chemical potential.

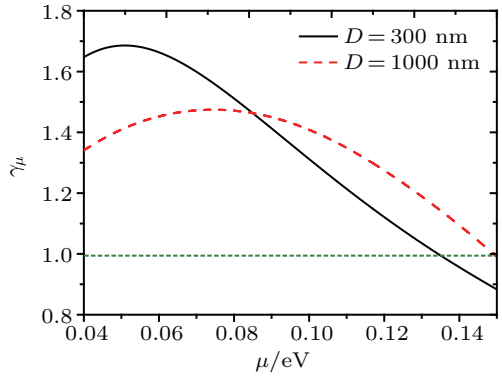


Fig. 4. (color online) Plots of normalized RTC with respect to chemical potential μ for vacuum gap $D = 300$ nm and 1000 nm. RTC is normalized to graphene-covered Si bulk.

Figure 4 shows that radiation transfer depends on the chemical potential and vacuum gap. Figure 5(a) shows the relationship between RTC and vacuum gap for different chemical potentials. The black solid, red dashed, and blue dotted curves correspond to RTC with chemical potentials of 0.05 eV, 0.075 eV, and 0.1 eV, respectively. The RTC is also normalized to that of graphene-covered Si bulk, and $\gamma_D = h(D)/h_{\mathrm{g-Si}}(D)$ is defined. For a given chemical potential, the value of γ_D first increases rapidly, and then decreases slowly with the increase of vacuum gap. The radiation transfer between graphene-covered Si bulks is dominated by SPs, and that between HMMs is dominated by HM. The variation behavior of the RTC curve shows that evanescent SPs play an important role in radiation transfer for smaller vacuum gaps, while HM contributes to the RTC importantly even when the vacuum gap is large. As the vacuum gap continues to increase, γ_D decreases. However, the radiation transfer between HMMs is still stronger than that between graphene-covered Si bulks. The values of RTC decline and the peak values shift toward the higher vacuum gaps when the chemical potential increases. Finally, we investigate the effect of the thickness of Si in HMM on RTC. Figure 5(b) shows the relationships between normalized RTC ($\gamma_d = h(d)/h_{\mathrm{g-Si}}(d)$) and thickness d for different chemical potentials. The distance between two HMMs is set to be $D = 300$ nm, and the calculation range of d is from 50 nm to 2000 nm. We use the transmission matrix method[37] rather than the EMT to obtain the reflection coefficient of HMMs because the EMT is valid only when $D > d$. Figure 5(b) shows that when the chemical potential is not extremely large, the radiation transfer between HMMs is always larger than that between graphene-covered Si bulks. Moreover, γ_d decreases as d increases. The value becomes 1.0 when d is sufficiently thick; thus, such an HMM structure is equivalent to a graphene-covered Si structure.

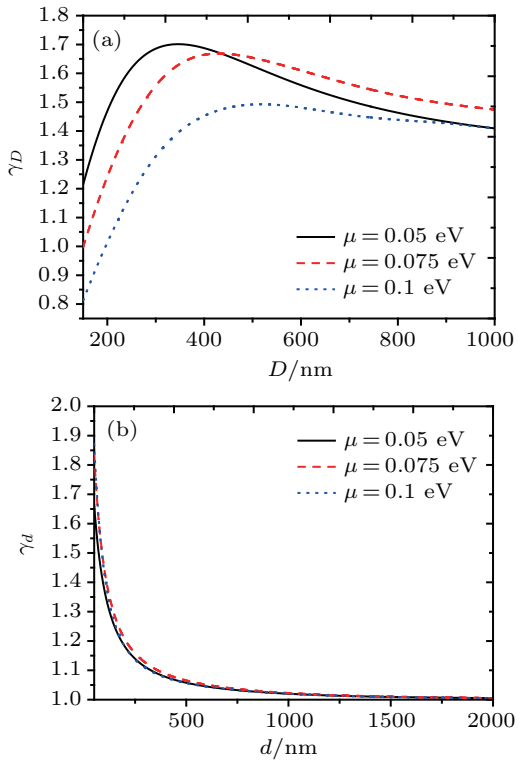


Fig. 5. (color online) Plots of normalized RTC as a function of (a) vacuum gap with $\mu = 0.05$ eV (black solid line), $\mu = 0.075$ eV (red dashed line), and $\mu = 0.1$ eV (blue dotted line). (b) Plots of RTC sets varying with dielectric thickness, where $D = 300$ nm.

Finally, we show the RTCs for HMMs (black dashed curve) and graphene-covered Si bulks (blue dotted line) as a function of temperature in Fig. 6. In both HMM and graphene-covered Si configurations, the chemical potentials and vacuum gaps are set to be 0.06 eV and 300 nm, respectively. It is shown that the RTCs of both configurations increase as the

temperature increases. Although the difference in RTC between HMM and graphene-covered Si bulk is very small in a low temperature range, the RTC between HMMs is larger than that between graphene-covered Si bulks in our studied temperature range. In addition, we also display the normalized RTC (red solid curve) as a function of temperature. We can see that the normalized RTC increases rapidly as the temperature increases at a lower temperature regime (< 150 K), while at higher temperature (> 150 K), the normalized RTC increases slowly and almost keeps constant. This means that the temperature has a more important effect on the RTC of the HMM configuration than that on the RTC of the graphene-covered Si configuration at lower temperature, which can also be seen from the comparison between the black dashed line and blue dotted line. Therefore, we can see that at room temperature HMM is better than graphene-covered Si bulk in enhancing near-field radiative heat transfer in the THz frequency range.

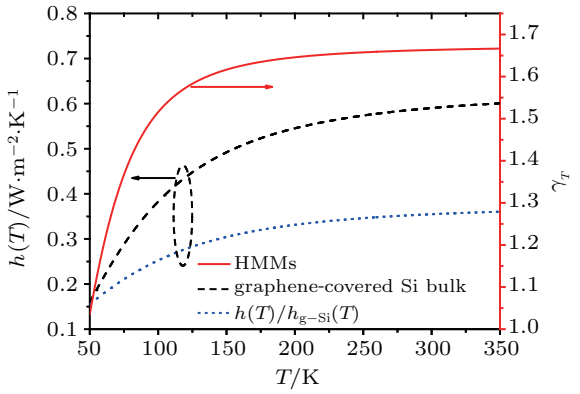


Fig. 6. (color online) RTCs for HMMs and graphene-covered Si bulks as well as normalized RTC as a function of temperature, with the chemical potential μ and vacuum gap D being 0.06 eV and 300 nm, respectively.

4. Conclusion

We propose graphene-based hyperbolic metamaterials to investigate the contribution of THz wave on the near-field radiative heat transfer. We find that due to the existence of the hyperbolic mode in the HMM, the THz radiative heat transfer in some frequency ranges can be enhanced remarkably compared with that between graphene-covered Si bulks. Even in the whole THz frequency range, the radiative transfer coefficient can also be enhanced. More importantly, the near-field radiative heat transfer in the THz band can be actively controlled by changing the chemical potential of graphene. We also show that when the width of Si is sufficiently large, the radiation transfer coefficient of HMM is equal to that of graphene-covered Si bulk. We believe that the results obtained in this study are useful for actively controlling the energy transfer in the THz frequency regime.

References

[1] Wilde Y D, Formanek F, Carminati R, Gralak B, Lemoine P A, Joulain K, Mulet J P, Chen Y and Greffet J J 2006 *Nature* **444** 740
[2] Kittel A, Wischnath U, Welker J, Huth O, Rüting F and Biehs S A 2008 *Appl. Phys. Lett.* **93** 193109
[3] Huth F, Schnell M, Wittborn J, Ocelic N and Hillenbr R 2011 *Nat. Mater.* **10** 352
[4] Worbes L, Hellmann and Kittel A 2013 *Phys. Rev. Lett.* **110** 134302
[5] Raman A P, Anoma M A, Zhu L, Rephaeli E and Fan S 2014 *Nature* **515** 540
[6] Laroche M, Carminati R and Greffet J J 2006 *J. Appl. Phys.* **100** 063704
[7] Narayanaswamy A and Chen G 2003 *Appl. Phys. Lett.* **82** 3544
[8] Messina R and Ben-Abdallah P 2013 *Sci. Rep.* **3** 1383
[9] Biehs S A, Tschikin M, Messina R and Ben-Abdallah P 2013 *Appl. Phys. Lett.* **102** 131106
[10] Biehs S A, Tschikin M, Messina R and Ben-Abdallah P 2012 *Appl. Phys. Lett.* **109** 104301
[11] Shen S, Narayanaswamy A and Chen G 2009 *Nano Lett.* **9** 2909
[12] Biehs S A, Ben-Abdallah P, Rosa F S S, Joulain K and Greffet J J 2011 *Opt. Express* **19** A1088
[13] Demtröder W 2008 *Laser Spectrosc.: Vol 1: Basic Principles 4th edition* (Berlin: Springer)
[14] Ferguson B and Zhang X C 2002 *Nat. Mater.* **1** 26
[15] Landy N I, Bingham C M, Tyler T, Jokerst N, Smith D R and Padilla W J 2009 *Phys. Rev. B* **79** 125104
[16] Anker J N, Hall W P, Lyandres O, Shah N C, Zhao J and Van Duyne R P 2008 *Nat Mater.* **7** 442
[17] Tonouchi M 2007 *Nat. Photon.* **1** 97
[18] Kuznetsov S A, Paulish A G, Gelf, A V, Lazorskiy P A and Fedorinin V N 2012 *Prog. Electromag. Res.* **122** 93
[19] Iwaszczuk K, Strikwerda A C, Fan K, Zhang X, Averitt R D and Jepsen P U 2012 *Opt. Express* **20** 635
[20] Liu X, Tyler T, Starr T, Starr A F, Jokerst N M and Padilla W J 2011 *Phys. Rev. Lett.* **107** 045901
[21] Liu N, Mesch M, Weiss T, Hentschel M and Giessen H 2010 *Nano Lett.* **10** 2342
[22] He X, Fujimura N, Lloyd J M, Erickson K J, Talin A A, Zhang Q, Gao W, Jiang Q, Kawano Y, Hauge R H, Léonard F and Kono J 2014 *Nano Lett.* **14** 3953
[23] Guo Y, Cortes C L, Molesky S and Jacob Z 2012 *Appl. Phys. Lett.* **101** 131106
[24] Kong B D, Sokolov V N, Kim K W and Trew R J 2010 *IEEE Sens. J.* **10** 443
[25] Andryieuski A, Lavrinenko A V and Chigrin D N 2012 *Phys. Rev. B* **86** 121108
[26] Falkovsky L A 2008 *J. Phys: Conf. Ser.* **129** 012004
[27] Novoselov K S, Geim A K, Morozov S V, Jiang D, Zhang Y, Dubonos S V, Grigorieva I V and Firsov A A 2004 *Science* **306** 666
[28] Berger C, Song Z, Li X, Wu X, Brown N, Naud C, Mayou D, Li T, Hass J, Marchenkov A N, Conrad E H, First P N and de Heer W A 2006 *Science* **312** 1191
[29] Stauber T, Peres N M R and Geim A K 2008 *Phys. Rev. B* **78** 085432
[30] Hu L and Chui S T 2002 *Phys. Rev. B* **66** 085108
[31] Smith D R and Schurig D 2003 *Phys. Rev. Lett.* **90** 077405
[32] Yeh P 1988 *Optical Waves in Layered Media* (New York: Wiley)
[33] Sayem A A, Rahman M M, Mahdy M R C, Jahangir I and Rahman M S 2016 *Sci. Rep.* **6** 25442
[34] Brundermann E, Hubers H W and Kimmitt M F G 2012 *Terahertz Techniques* (Berlin Heidelberg: Springer Series in Optical Sciences)
[35] Gusynin V P, Sharapov S G and Carbotte J P 2007 *J. Phys.: Condens. Matter* **19** 026222
[36] Zhang Z M 2007 *Nano/Microscale Heat Transfer* (New York: McGraw-Hill)
[37] Zhan T, Shi X, Dai Y, Liu X and Zi J 2013 *J. Phys: Condens. Matter* **25** 215301